Superlattices and Microstructures 111 (2017) 90–95

Contents lists available at ScienceDirect

Superlattices and Microstructures

journal homepage: www.elsevier.com/locate/superlattices

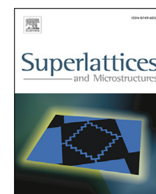

Correlation of TEM data with confined phonons to determine strain and size of Ge nanocrystals embedded in SixNy matrix

Rahim Bahariqushchi [a, *], Sinan Gündoğdu [a], Atilla Aydinli [b, 1]

[a] Bilkent University, Physics Department, Ankara, 06800, Turkey
[b] Uludag University, Electrical and Electronics Engineering Department, Bursa, 16059, Turkey

ARTICLE INFO

Article history:
Received 4 May 2017
Received in revised form 3 June 2017
Accepted 6 June 2017
Available online 7 June 2017

ABSTRACT

Models that use phonon confinement fail to provide consistent results for nanocrystal sizes in differing dielectric matrices due to varying stress experienced by nanocrystals in different dielectric environments. In cases where direct measurement of stress is difficult, the possibility of stress saturation as a function of size opens up a window for the use of phonon confinement to determine size. We report on a test of this possibility in Ge: Si_xN_y system. Ge nanocrystals (NCs) embedded in silicon nitride matrix have been fabricated using plasma enhanced chemical vapor deposition (PECVD) followed by post annealing in Ar ambient. Nanocrystal size dependence of Raman spectra was studied taking into account associated stress and an improved phonon confinement approach. Our analysis show same stress for NCs which have sizes below 7.0 nm allowing the use of phonon confinement to determine the nanocrystal size. The results are compared with TEM data and good agreement is observed.

© 2017 Elsevier Ltd. All rights reserved.

1. Introduction

Semiconductor nanocrystals (NCs) embedded in a wide band gap dielectric have attracted a lot of interest in the past decade, because of their tunable properties due to adjustable size and distribution, shape of NCs and the surrounding matrix [1–6]. Decreasing size of nanocrystals leads to quantum confinement of electrons (QCE) which in-turn results in tunable electrical and optical properties [6]. Size reduction also restricts the propagation of phonons, producing phonon confinement effects (PCE) modifying the vibrational modes of the NCs determined by their size, shape and the type of surrounding matrix. Raman scattering from NCs can give information about structure and size of NCs [7]. However, the application of Raman scattering in rapid determination of nanocrystal sizes in differing dielectric matrices remains a challenge. Phonon confinement model (PCM) was used as early as 1981 [8] to describe Raman shift and lineshape for Si NCs which were previously observed by two groups [9,10]. The reports showed shift of Raman line towards the red as a function of decreasing NC size and broadening of Raman spectra with respect to bulk silicon. Richter et al. [8] explained these observations based on relaxation of q-vector selection rule for the excitation of the Raman active optical phonons due to the small crystallite size which leads to phonon confinement in NCs [8]. Based on Heisenberg uncertainty, Richter et al. developed the PCM which later was generalized for different types of NCs by Fauchet in 1986 [11]. Different PCMs for Si NCs is still being developed by several

* Corresponding author.
E-mail address: rahim.qushchi@fen.bilkent.edu.tr (R. Bahariqushchi).
[1] Formerly at Bilkent University, Physics Department, Ankara, 06800 Turkey.

http://dx.doi.org/10.1016/j.spmi.2017.06.020
0749-6036/© 2017 Elsevier Ltd. All rights reserved.

groups to improve the agreement with experimental data [12–17]. The PCM have also been applied to the analysis of Ge NCs [7], and further developed by several groups [18–23]. In this work, we apply the improved PCM developed in Ref. [23] for Ge NCs embedded in Si_xN_y matrix to determine size and correlating with transmission electron microscopy data.

Among many NCs, Ge NCs seems to have many advantages over other alternative semiconductors, because of its compatibility with silicon technology and also due to its stronger QCE compared with Si which leads to easier tunability of its band gap. Stronger QCE in Ge compared with Si comes from larger exciton Bohr radius and smaller effective mass of charge barriers in Ge [24,25]. Other advantages of Ge NCs over Si is lower melting point which reduces the cost of crystallization during the annealing process. However, indirect nature of Ge fundamental band gap makes its use as an active photonic device impossible, with traditional approaches [26]. There have been a lot of effort to overcome this problem. Controlled stress can give an important degree of freedom for band gap engineering. Strain modifies the lattice constant and therefore, can modify the band gap which in turn can lead to direct band gap behavior [26]. The difference between the direct and indirect band gaps of bulk Ge is only 140 meV [27] and it is known that tensile strain induces a reduction of the direct band gap faster than the reduction of the indirect band gap. While the total strain required to make Ge direct band gap is large (1.9%), it is suggested that tensile strain along with heavy n-type doping ($>2 \times 10^{19}$ cm^{-3}) filling the indirect minima may lead to pseudo direct material [27]. Using this method, direct gap optical gain from Ge on Si have been measured [28]. Recently, two dimensional Ge nanomembranes have been shown to emit efficient light [26] under biaxial tensile strain of up to 2%. Decreasing the size of Ge down to a few nanometers can also lead to direct band gap [1]. Yuan et al. [29] have used stress manipulating for band gap engineering of Si NCs. They showed a strain induced phase transition of microstructure of NCs from cubic to hexagonal structure under strong compressive strain. These two microstructures display different band gaps, and as a result, a red shift in photoluminescence peak of microstructure with hexagonal structure was observed. Liu et al. [30] also provided theoretical calculations showing effect of stress distribution on physical and thermodynamical properties of NCs. Wada et al. [31] also proposed a high performance photodetector based on tuning the band gap by manipulating stress on Ge NCs.

For practical use of Ge NCs in photovoltaics, optoelectronics, memory and thermoelectric devices, it is crucial to understand and control the structural details of Ge NCs embedded in various matrices, as details of the structure, such as concentration, size, shape, type of embedded matrix and stress state, dictate the final optical and electrical performance of devices. Raman scattering have been widely used for studying stress and size of NCs [7,32]. This method provides a nondestructive method to determine size and size distribution of nanocrystals. Separating the opposing shifts of compressive stress and phonon confinement, here we report on a test of an improved model for phonon confinement [23] for Ge NCs embedded in silicon nitride matrix.

2. Experiment

All sets of samples were grown using plasma enhanced chemical vapor deposition (PECVD) method. Growths have been done in a PECVD reactor (model PLASMALab 8510C) on quartz and Si substrates. For growing SiGeN films, we used 100 sccm SiH_4 (2% in N_2), 30 sccm NH_3 and varying GeH_4 (2% in He) flow rate ranging from 25 to 150 sccm. The process pressure was 1000 mbar, RF power was 12 W and sample temperature was 250 C. Single layers of SiGeN samples with thickness around 200 nm were grown on Si substrates and Ge content varying from 4% to 24%. All sets of samples were followed by thermal annealing in Ar atmosphere from 700 C to 900 C for 30 min to form germanium NCs. Thickness and optical parameters of samples were studied using variable angle spectroscopic ellipsometry. Ge NC sizes of some samples were measured using transmission electron microscopy (TEM).

Compositional analysis have been done using Rutherford backscattering spectrometry (RBS), with a 2.0 MeV He^+ beam in glancing detection configuration (backscattering angle of 105°) and using SIMNRA software. Ge concentration was found to be between 4% and 24% for the samples grown. Raman spectroscopy was performed for all samples using Ar ion laser at 514.5 nm and a high resolution double monochromator with CCD detection to study the degree of Ge crystallization as well as the position and lineshape of the Raman phonon line as a function of size. Here, cross polarized configuration has been used to eliminate the signal off of the (100) Si surface to suppress the signal from substrate.

3. Results and discussion

The amount of Ge in the silicon nitride film is critical in the formation of Ge NCs. We, therefore, used Rutherford backscattering spectroscopy to determine composition of as grown thin films of SiXNy:Ge layers. RBS spectrum shows clear signatures of Ge, Si and N. The data has been fit to determine the Ge content in the silicon nitride matrix. The N signal does not vary with increasing Ge content as opposed to Si which is replaced with Ge. Ge content found to range between 4% and 24%.

Thin SixNy:Ge films with Ge content varied from 4% to 24% annealed at 900 °C. Samples with 4% and 9% Ge show no crystallization when annealed at 900 C. Ge content threshold for crystallization under these annealing conditions is found to be around 15% Ge in SixNy films (see Fig. 1).

Even at this Ge value, Raman spectra shows a very broad band which is an indication of small Ge NCs and nonuniform NCs distribution. Sample with 24% Ge, however, shows a narrow and strong peak demonstrating larger NCs with uniform size distribution. We select samples with 24% Ge content for further study. Fig. 2b shows HRTEM micrograph of the sample with 24% Ge annealed at 900C. Crystal planes are well formed in the sample. Fig. 3 shows Raman spectra for samples with 24% Ge

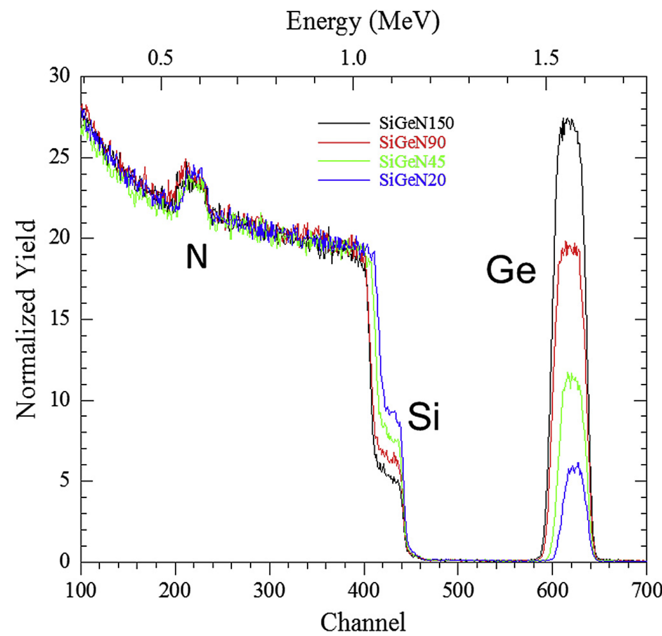

Fig. 1. Figure shows the RBS data in the 0.3–1.8 MeV energy range from as grown films of SixNy:Ge. Samples are labeled according to increasing flow rate of GeH_4 gas from blue to black. (For interpretation of the references to colour in this figure legend, the reader is referred to the web version of this article.)

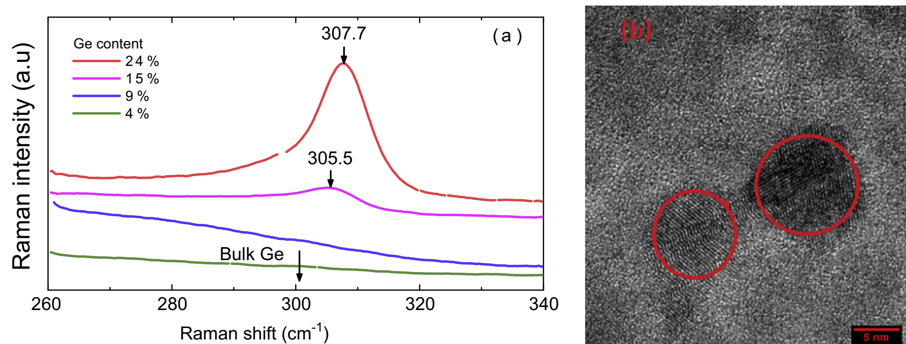

Fig. 2. Raman spectra for samples with varying Ge content ranging from 4% to 24% in SixNy matrices annealed at 900C for 30 min. a) and HRTEM micrograph of the sample with 24% Ge, b). Crystallographic planes as well as associated line defects are well resolved.

annealed under different conditions. All samples show blueshift with respect to bulk Ge. Larger NCs also show larger blueshift. Total Raman shift with respect to bulk Ge can be understood in terms of combination of redshift due to phonon confinement effect and blueshift caused by compressive stressexerted by the dense Si_xN_y matrix. Strain measurement on Ge NCs embedded in SiO_2 matrix have been done by Paillard et al. [7] using Raman spectroscopy and HRTEM micrographs. They observed strong compressive stress induced by surrounding matrix. For calculating strain, they measured Raman shift for NCs with sizes between 11.0 and 14.5 nm, phonon confinement induced shift is negligible and all the observed Raman shift can be attributed to strain induced shift. They observed size-independent strain for NCs with sizes below 14.5 nm. They applied this constant strain induced shift to all samples for analysing Raman spectra. They also suggest as the origin of this strain to be due to liquid-solid phase transition of Ge during cooling. Strain on Ge NCs embedded in SiO_2 and Si_3N_4 also is measured in Ref. [33]. They used a complementary metal oxide-semiconductor-compatible process (CMOS) with SiO_2 and Si_3N_4 layers and produce Ge NCs with sizes between 23 and 110 nm. In this size regime, the phonon confinement effects are negligible and all of the observed Raman shift can be attributed to stress effect. Their analysis show a size dependent tensile stress of 0.5%–1% and compressive stress of 0.7%–4.5% for Ge NCs embedded within SiO_2 and Si_3N_4, respectively. This stress is inversely size dependent in NCs [7,33]. However, for sizes below a critical value, it can be assumed to be constant [7,33]. Phonon confinement effect (PCE) is also inversely size dependent [7]. Assuming constant blue shift for all samples and inversely size dependent PCE, a total blue shift is predicted which was found to be in good agreement with average size of NCs obtained from TEM results.

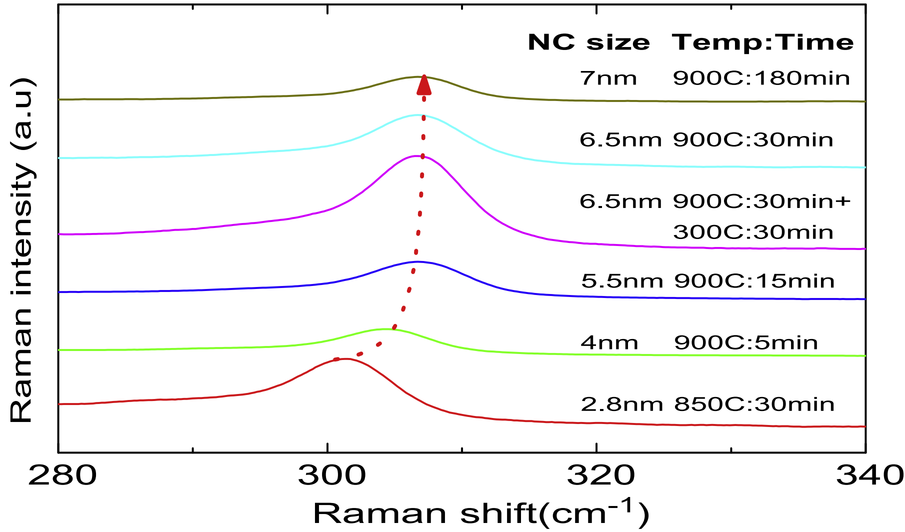

Fig. 3. Size dependent Raman shift. Stress induced shift can be calculated from the difference between these experimental data and phonon confinement induced shift predicted by equation (5).

In conventional PCM, the phonon wave function has the form [23]:

$$\Psi(r) = A_q \exp(-\alpha r^2/L^2)\exp(-iqr) \tag{1}$$

where q is the phonon wave vector, L is diameter of NCs and "α" is a dimensionless parameter indicating degree of confinement of phonons to the center of NCs. The relation between Raman peak shift and NC size provides the possibility of determining NC size via Raman spectroscopy. However, there are problems using formula (1) for analysing the size of NCs: Phonon wave function suggested by formula (1) is ambiguous and "α" value is arbitrary. Based on works by Refs. [11] and [34] the parameters were determined as: $\alpha = 8\pi^2$ or $\alpha = 9.67$. These values are frequently used by groups as default values, during the use of equation (1) in Raman analysis of NCs. However, as can be seen from equation (1), L is part of the combination (α/L^2) in PCM and as a result NC size value inherently depends on the value of "α". Therefore, using PCM for "α". Independent determination of NC size is not possible.

The relationship between Raman peak shift and NC size is obtained taking into account the discretness of NCs lattice vibrations [23]. In NCs much smaller than the phonon mean free path, phonons experience several reflection and scattering on NCs surfaces during phonon life time. This leads to standing waves for vibrational eigenmodes of NCs instead of traveling waves. A simple model of N atoms in one dimension is proposed to take into account the discretness of NCs vibration. Eigenmodes of this simple system is simply given by:

$$\omega_s = 2\,(k/m)^{1/2}\,\mathrm{Sin}(q_s\,a/2) \tag{2}$$

where $q_s = \pi s/aN$, $S = 1,2, \ldots, N-1$.

The maximum wave vector of this system with infinite length is $q = \pi/a$. However, for finite sizes, the maximum possible wave vector will be smaller than infinite case and it will differ from reciprocal wave vector π/a by;

$$\Delta q = \pi/L+a. \tag{3}$$

where L is the dimension of NCs. For small NCs this change is considerable. By generalizing this relation to three dimensions and Taylor expansion of ω with respect to q and using this simple dispersion relation for optical phonon mode:

$$\omega(q) = A + B\cos(qa) \tag{4}$$

we get:

$$\Delta\omega = -(3\pi^2 a^2 B/2(L+a)^2) \tag{5}$$

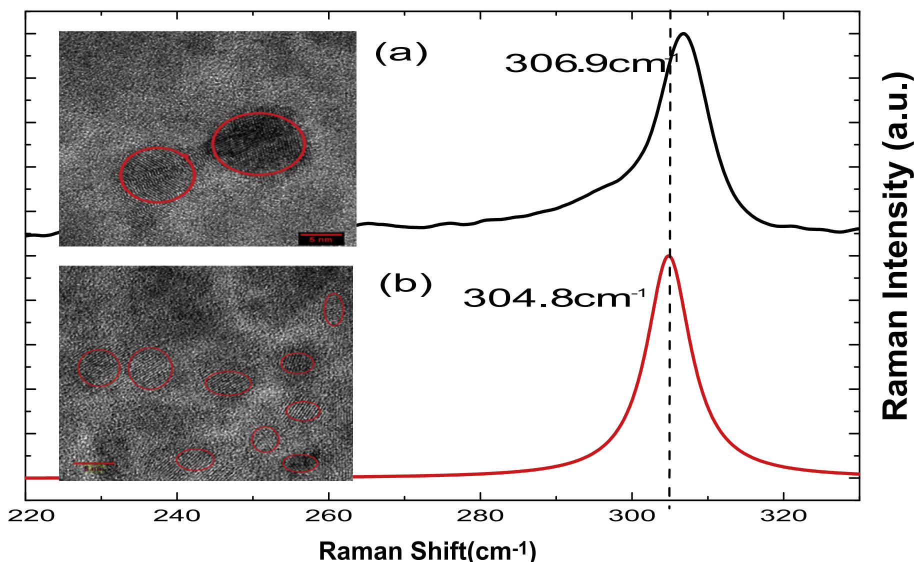

Fig. 4. HRTEM and Raman spectra for samples annealed at 900C for a) 30 min and b) 5 min. Sample annealed for longer time shows larger NCs.

where a is the lattice constant, L is NC diameter and B is a parameter which is calculated for germanium to be 18.6 cm^{-1}. B is calculated by comparing the Ge NCs sizes obtained from methods like XRD, TEM. Equation (5) gives a relationship between the displacement of Raman peak position and the size of nanocrystals for crystals with a cubic lattice (diamond, silicon, germanium). The proposed model does not include any adjustable parameters, unlike the conventionally used phonon confinement model (PCM) and can be employed for estimation of NCs sizes.

Fig. 4 shows HRTEM micrograph and Raman spectra of samples annealed at 900C for 30 and 5 min. Average Ge NC size is determined using TEM micrographs and determined to be 6.5 nm for the sample annealed for 30 min and 4.0 nm for the sample annealed for 5 min. Raman peak shift for sample (a) and (b) are 306.9 cm^{-1} and 304.8 cm^{-1} respectively. These values show 6.2 cm^{-1} and 4.1 cm^{-1} blueshift with respect to bulk Ge peak which is at 300.7 cm^{-1} [35]. These shifts are combinations of stress induced and phonon confinement induced shifts. In order to analyse the size of the NCs from Raman spectra, we need to separate the shifts caused by phonon confinement and stress. To deduce the shift induced by phonon confinement, we used equation (5). For the determination of NC size, we use the values obtained from HRTEM micrographs.

For sample (a) with NCs diameter of 6.5 nm, from equation (5), we obtain, $\Delta\omega_{PCM} = -1.8$ cm^{-1} where we used a = 5.66 Å for Ge lattice constant, L = 6.5 nm for NC size and B = 18.6 cm^{-1}. Thus, stress induced shift can easily be calculated using $\Delta\omega_{strain} = \Delta\omega_{Tot} - \Delta\omega_{PCM} = 6.2 + 1.8 = 8.0$ cm^{-1}.

The same approach, for sample (b) with NCs size 4.0 nm, phonon confinement model gives: $\Delta\omega_{PCM} = -4.1$ cm^{-1} and stress induced shift is calculated to be, $\Delta\omega_{strain} = \Delta\omega_{Tot} - \Delta\omega_{PCM} = 4.1 + 4.1 = 8.2$ cm^{-1}.

These results show that almost the same amount of stress induced shift exists for NCs with different sizes. Conversely, assuming the same stress induced shift one can unambiguously determine NC size from PCM using Raman spectroscopy. This result is in agreement with results of [7,33] where, using CMOS lithographic processes to create nano-cylindrical pillars to size limit the multi-layer, sequential deposited SiGe films, proposed that in small Ge NC regime, stress induced shift can be considered constant for different sizes of Ge NCs embedded in SiO_2 or Si_3N_4. By considering this constant value for stress induced shift (around 8 cm^{-1} for our samples) and equation (5), it is possible to get NCs size from Raman spectra. We have done this for all samples and results are in good agreement with results obtained from HRTEM graphs.

4. Conclusions

Raman spectra of Ge NCs embedded in SixNy matrices have been analysed taking into account phonon confinement and stress induced shifts, separately. To differentiate the shift induced by phonon confinement and stress we have used a model developed by Ref. [23] for phonon confinement induced shifts. Size of NCs have been obtained using HRTEM cross section micrographs to be used in the calculation NC size from the PCM. Using experimental Raman shift and values calculated from phonon confinement, we obtain the stress induced Raman shift for samples with different NCs sizes. This stress induced shift was almost the same for all NCs sizes, in our samples. This result is in agreement with results of several groups [7,33] who used CMOS processes to limit NC sizes and assumed constant stress induced shift for small NCs. This method gives us an unambiguous tool for estimating NC sizes from Raman spectra. By assuming this constant value for stress induced shift (~8 cm^{-1}) and the proposed PCM, we calculated NCs size for different samples and results are in good agreement with those obtained from HRTEM graphs.

Acknowledgements

We would like to sincerely thank Dr. Salvatore Mirabella of University of Catania and CNR-IMM for RBS measurements and Dr.Sinan Balci for fruitfull discussions. The authors acknowledge use of the services and facilities of UNAM-National Nanotechnology Research Center at Bilkent University.

References

[1] L. Pavesi, L. Dal Negro, Ca Mazzoleni, G. Franzo, F. Priolo, Optical gain in silicon nanocrystals, Nature 408 (6811) (2000) 440–444.
[2] Gavin Conibeer, Martin Green, Eun-Chel Cho, Dirk König, Young-Hyun Cho, Thipwan Fangsuwannarak, Giuseppe Scardera, et al., Silicon quantum dot nanostructures for tandem photovoltaic cells, Thin Solid Films 516 (20) (2008) 6748–6756.
[3] Eun-Chel Cho, Martin A. Green, Gavin Conibeer, Dengyuan Song, Young-Hyun Cho, Giuseppe Scardera, Shujuan Huang, et al., Silicon quantum dots in a dielectric matrix for all-silicon tandem solar cells, Adv. OptoElectron. 2007 (2007).
[4] S. Mirabella, S. Cosentino, A. Gentile, G. Nicotra, N. Piluso, L.V. Mercaldo, F. Simone, C. Spinella, A. Terrasi, Matrix role in Ge nanoclusters embedded in Si3N4 or SiO2, Appl. Phys. Lett. 101 (1) (2012) 011911.
[5] S. Cosentino, A.M. Mio, E.G. Barbagiovanni, R. Raciti, R. Bahariqushchi, M. Miritello, G. Nicotra, et al., The role of the interface in germanium quantum dots: when not only size matters for quantum confinement effects, Nanoscale 7 (26) (2015) 11401–11408.
[6] Y.M. Niquet, G. Allan, C. Delerue, M. Lannoo, Quantum confinement in germanium nanocrystals, Appl. Phys. Lett. 77 (8) (2000) 1182–1184.
[7] A. Wellner, V. Paillard, C. Bonafos, H. Coffin, A. Claverie, B. Schmidt, K.H. Heinig, Stress measurements of germanium nanocrystals embedded in silicon oxide, J. Appl. Phys. 94 (9) (2003) 5639–5642.
[8] H. Richter, Z.P. Wang, L. Ley, The one phonon Raman spectrum in microcrystalline silicon, Solid State Commun. 39 (5) (1981) 625–629.
[9] J.F. Morhange, G. Kanellis, M. Balkanski, Raman study of laser annealed silicon, Solid State Commun. 31 (11) (1979) 805–808.
[10] R. Tsu, M. Izu, S.R. Ovshinsky, F.H. Pollak, Electroreflectance and Raman scattering investigation of glow-discharge amorphous Si: F: H, Solid State Commun. 36 (9) (1980) 817–822.
[11] I.H. Campbell, Ph M. Fauchet, The effects of microcrystal size and shape on the one phonon Raman spectra of crystalline semiconductors, Solid State Commun. 58 (10) (1986) 739–741.
[12] V. Paillard, P. Puech, M.A. Laguna, R. Carles, B. Kohn, F. Huisken, Improved one-phonon confinement model for an accurate size determination of silicon nanocrystals, J. Appl. Phys. 86 (4) (1999) 1921–1924.
[13] V.A. Volodin, V.A. Sachkov, Improved model of optical phonon confinement in silicon nanocrystals, J. Exp. Theor. Phys. 116 (1) (2013) 87–94.
[14] Giuseppe Faraci, Santo Gibilisco, Agata R. Pennisi, Carla Faraci, Quantum size effects in Raman spectra of Si nanocrystals, J. Appl. Phys. 109 (7) (2011) 074311.
[15] Iain F. Crowe, Matthew P. Halsall, Oksana Hulko, Andrew P. Knights, Russell M. Gwilliam, Maciej Wojdak, Anthony J. Kenyon, Probing the phonon confinement in ultrasmall silicon nanocrystals reveals a size-dependent surface energy, J. Appl. Phys. 109 (8) (2011) 083534.
[16] Patrice Miska, et al., Embedded silicon nanocrystals studied by photoluminescence and Raman spectroscopies: exciton and phonon confinement effects, J. Phys. Chem. C 114.41 (2010) 17344–17349.
[17] G. Faraci, S. Gibilisco, P. Russo, A.R. Pennisi, S. La Rosa, Modified Raman confinement model for Si nanocrystals, Phys. Rev. B 73 (3) (2006) 033307.
[18] X.L. Wu, T. Gao, X.M. Bao, F. Yan, S.S. Jiang, D. Feng, Annealing temperature dependence of Raman scattering in Ge+-implanted SiO 2 films, J. Appl. Phys. 82 (5) (1997) 2704–2706.
[19] E.B. Gorokhov, V.A. Volodin, D.V. Marin, D.A. Orekhov, A.G. Cherkov, A.K. Gutakovskii, V.A. Shvets, A.G. Borisov, M.D. Efremov, Effect of quantum confinement on optical properties of Ge nanocrystals in GeO2 films, Semiconductors 39 (10) (2005) 1168–1175.
[20] S.R.C. Pinto, A.G. Rolo, A. Chahboun, Reza J. Kashtiban, U. Bangert, M.J.M. Gomes, Raman study of stress effect on Ge nanocrystals embedded in Al 2 O 3, Thin Solid Films 518 (19) (2010) 5378–5381.
[21] J.E. Chang, P.H. Liao, C.Y. Chien, J.C. Hsu, M.T. Hung, H.T. Chang, S.W. Lee, et al., Matrix and quantum confinement effects on optical and thermal properties of Ge quantum dots, J. Phys. D Appl. Phys. 45 (10) (2012) 105303.
[22] V.A. Volodin, D.V. Marin, V.A. Sachkov, E.B. Gorokhov, Hervé Rinnert, Michel Vergnat, Applying an improved phonon confinement model to the analysis of Raman spectra of germanium nanocrystals, J. Exp. Theor. Phys. 118 (1) (2014) 65–71.
[23] A.P. Meilakhs, S.V. Koniakhin, New Explanation of Raman Peak Redshift in Nanoparticles, arXiv preprint arXiv:1602.00114, 2016.
[24] Yoshihito Maeda, Visible photoluminescence from nanocrystallite Ge embedded in a glassy SiO 2 matrix: evidence in support of the quantum-confinement mechanism, Phys. Rev. B 51 (3) (1995) 1658.
[25] Toshihide Takagahara, Kyozaburo Takeda, Theory of the quantum confinement effect on excitons in quantum dots of indirect-gap materials, Phys. Rev. B 46 (23) (1992) 15578.
[26] Jose R. Sánchez-Pérez, Cicek Boztug, Feng Chen, Faisal F. Sudradjat, Deborah M. Paskiewicz, R.B. Jacobson, Max G. Lagally, Roberto Paiella, Direct-bandgap light-emitting germanium in tensilely strained nanomembranes, Proc. Natl. Acad. Sci. 108 (47) (2011) 18893–18898.
[27] Xiaochen Sun, Jifeng Liu, Lionel C. Kimerling, Jurgen Michel, Direct gap photoluminescence of n-type tensile-strained Ge-on-Si, Appl. Phys. Lett. 95 (1) (2009) 011911.
[28] Jifeng Liu, Lionel C. Kimerling, Jurgen Michel, Monolithic Ge-on-Si lasers for large-scale electronic–photonic integration, Semicond. Sci. Technol. 27 (9) (2012) 094006.
[29] C. Yuan, Q. Liu, B. Xu, Strain-induced structural phase transition of Si nanoparticles, J. Phys. Chem. C 115 (33) (2011) 16374–16377.
[30] L. Liu, K.L. Teo, Z.X. Shen, J.S. Sun, E.H. Ong, A.V. Kolobov, Y. Maeda, Raman scattering investigation of a G e/S i O 2/Si nanocrystal system under hydrostatic pressure, Phys. Rev. B 69 (12) (2004) 125333.
[31] Y. Ishikawa, K. Wada, D.D. Cannon, J. Liu, H.C. Luan, L.C. Kimerling, Strain-induced band gap shrinkage in Ge grown on Si substrate, Appl. Phys. Lett. 82 (13) (2003) 2044–2046.
[32] S.R.C. Pinto, A.G. Rolo, A. Chahboun, R.J. Kashtiban, U. Bangert, M.J.M. Gomes, Raman study of stress effect on Ge nanocrystals embedded in Al 2 O 3, Thin Solid Films 518 (19) (2010) 5378–5381.
[33] Po-Hsiang Liao, Ting-Chia Hsu, Kuan-Hung Chen, Tzu-Hsuan Cheng, Tzu-Min Hsu, Ching-Chi Wang, Tom George, P.W. Li, Size-tunable strain engineering in Ge nanocrystals embedded within SiO2 and Si3N4, Appl. Phys. Lett. 105 (17) (2014) 172106.
[34] J. Zi, K. Zhang, X. Xie, Comparison of models for Raman spectra of Si nanocrystals, Phys. Rev. B 55 (15) (1997) 9263.
[35] J.H. Parker Jr., D.W. Feldman, M. Ashkin, Raman scattering by silicon and germanium, Phys. Rev. 155 (3) (1967) 712.